GEM NEWS INTERNATIONAL

Contributing Editors
Gagan Choudhary, Gem Testing Laboratory, Jaipur, India (gagan.choudhary@iigjrlc.org)
Christopher M. Breeding, GIA, Carlsbad (christopher.breeding@gia.edu)
Guanghai Shi, School of Gemmology, China University of Geosciences, Beijing (shigh@cugb.edu.cn)

COLORED STONES AND ORGANIC MATERIALS

Atypical "box bead" cultured pearls. Gemologists are aware of two main types of bead cultured pearls—bead cultured (BC) and atypical bead cultured (aBC). BC pearls are cultured with the typical round, predominantly freshwater shell bead nuclei, while aBC pearls are cultured with any material that is not typical. Atypical bead nuclei include fancy-shaped shell beads, pearls of any kind, plastic beads, gemstones, or other materials of various shapes. GIA's Bangkok laboratory received five loose undrilled pearls as research samples for examination. These were reportedly sold as "tissue box pearls" in the Indian market by a trader known to some GIA staff. Externally they exhibited a smooth surface with luster resembling that of South Sea *Pinctada maxima* cultured pearls. The samples ranged from 8.00 × 7.26 × 6.05 mm to 9.93 × 7.86 × 5.86 mm, weighing between 2.50 and 3.49 ct, and exhibited a baroque form with a white to cream color (figure 1).

Microradiographic examination revealed unusual box-shaped demarcation outlines uncharacteristic of traditional BC pearls (figure 2). To the author's knowledge, this kind of internal rectangular shape is never seen in natural pearls. Sample 2 revealed an additional structural feature extending from the shorter side of the "box bead" (see red arrow in figure 2). Sample 3 possessed two distinct radio-translucent areas around the box-shaped outline; these are expected for voids or certain organic-rich features in pearls. Samples 4 and 5 also showed similar radio-translucent features, but to a lesser extent. Since the rectangular internal structures are not observed in natural pearls, the clear demarcation features with a box-shaped outline are enough to identify these as aBC pearls.

The box-shaped beads clearly influenced the external shapes of their pearl hosts when they formed within the mollusks, as seen in figure 1. Samples 2 and 3 were cut in half for further examination of their internal structures. Under magnification, each half showed an obvious demarcation between the box-shaped bead and the nacre overgrowth. The "box beads" appeared to be more translucent than traditional beads and exhibited platy structure and banding in some areas, proving they were fashioned from shell. Additionally, the feature in sample 2 possessed a radial structure and appeared somewhat translucent. Observation through a gemological microscope revealed that the gaps around the nucleus in sample 3 were in fact voids with areas of dark organic-rich material, likely conchiolin, present within (figure 3).

Another point of interest was the inert reaction of the shell nuclei in each half of both samples under optical X-

Figure 1. The five "box bead" cultured pearls examined ranged from 8.00 × 7.26 × 6.05 mm to 9.93 × 7.86 × 5.86 mm. Photo by Lhapsin Nillapat.

Editors' note: Interested contributors should send information and illustrations to Stuart Overlin at soverlin@gia.edu or GIA, The Robert Mouawad Campus, 5345 Armada Drive, Carlsbad, CA 92008.

Gems & Gemology, Vol. 58, No. 3, pp. 378–398.

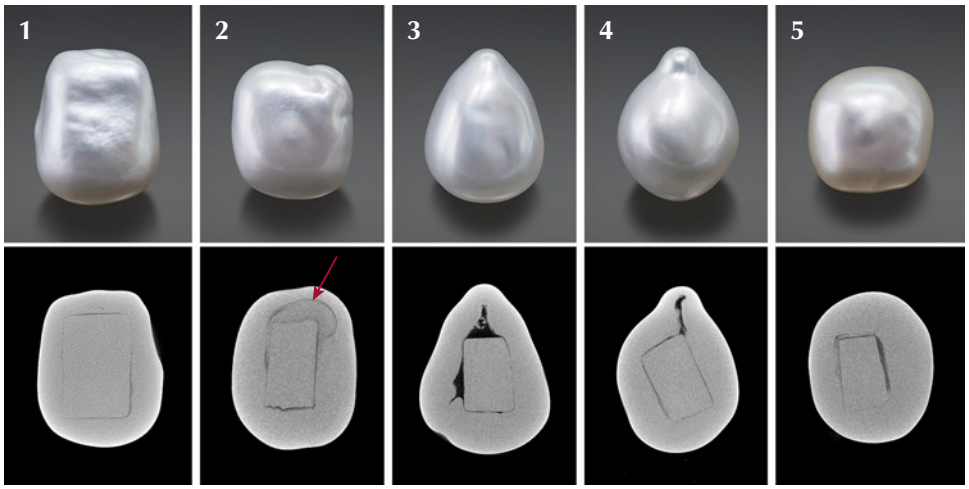

Figure 2. The five "box bead" cultured pearls (top) together with their X-ray computed microtomography (μ-CT) slices showing the obvious rectangular bead demarcations resembling a box shape (bottom). The red arrow indicates the additional structural feature observed within sample 2. Photos by Lhapsin Nillapat.

ray fluorescence. Since most freshwater bead nuclei show strong yellowish green or greenish yellow reactions, it was clear that the "box beads" were not fashioned from freshwater mussel shells.

Energy dispersive X-ray fluorescence (EDXRF) results of the "box bead" nuclei, outer nacre layers, and the radial calcitic area revealed major amounts of calcium, along with high levels of strontium ranging from 1209 to 1986 ppm, and manganese below 63 ppm. The low levels of manganese detected by EDXRF corresponded to the inert optical X-ray fluorescence reaction (figure 4), as the intensity of any reaction is directly correlated to the manganese levels (P. Kessrapong et al., "Atypical bead cultured *Pinctada maxima* pearls nucleated with freshwater non-bead cultured pearls," *GIA Research News*, April 6, 2020, https://www.gia.edu/gia-news-research/atypical-bcp-nucleated-with-nbcp). The high strontium and low manganese concentrations indicated saltwater origin.

Under long-wave ultraviolet radiation, the sawn surfaces exhibited a bluish reaction. Sample 2 showed additional very weak orangy reactions associated with the columnar feature partially surrounding the bead (figure 5).

Short-wave UV fluorescence spectra were also collected from the pearl surfaces using a GIA-developed spectrometer. The spectra showed two distinct peaks around 330 and 360 nm with counts above 10,000, indicating the surfaces were not processed using bleach or any whitening/brightening agents (C. Zhou et al., "Detection of color treatment and optical brightening in Chinese freshwater 'Edison' pearls," Summer 2021 *G&G*, pp. 124–133).

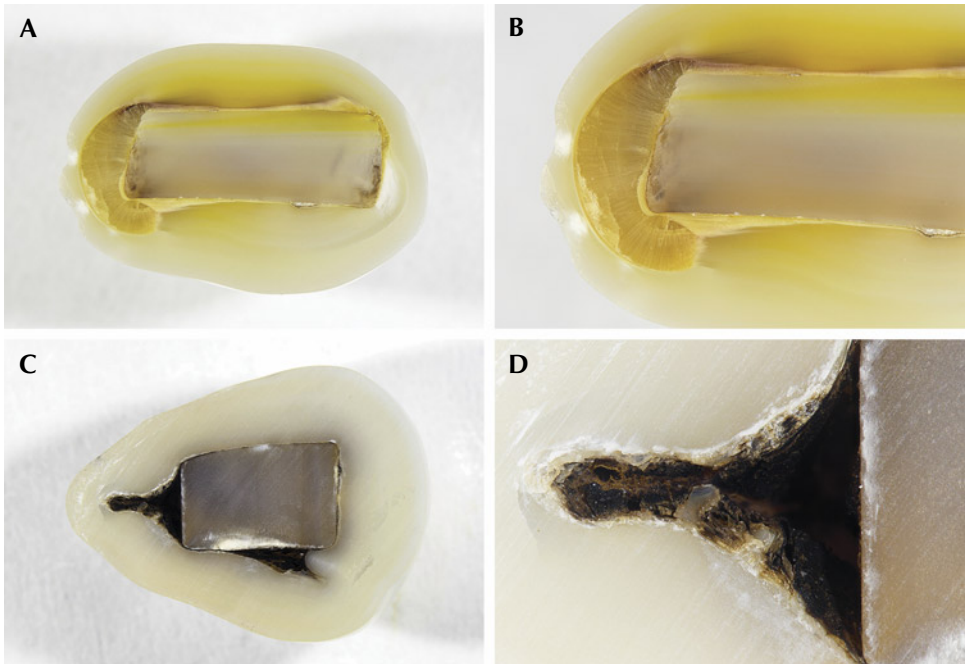

Figure 3. A: Cross section of sample 2. B: Radial columnar structures, identified as calcite by Raman, observed in an area within the nacre overgrowth covering sample 2's bead nucleus. C: Cross section of sample 3. D: Magnified view of one of the void features with dark organic-rich material attached to the inner surface. Photos by Ravenya Atchalak; fields of view 14.40 mm (A and C), 7.20 mm (B), and 2.88 mm (D).

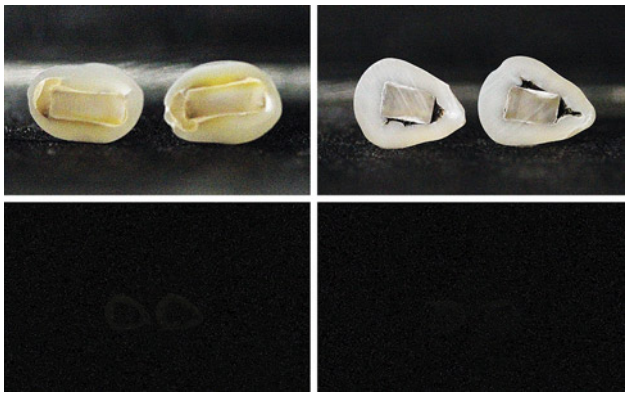

Figure 4. The cross sections of sample 2 (top left) and sample 3 (top right) under white light and their inert reactions under X-ray fluorescence (bottom). Photos by Ravenya Atchalak.

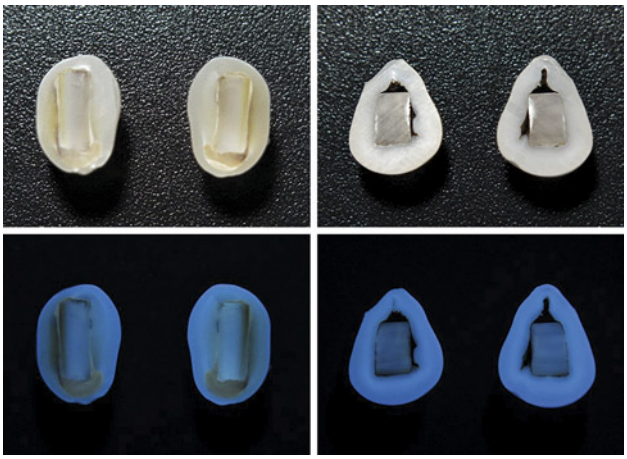

Figure 5. The cross sections of sample 2 (top left) and sample 3 (top right) under white light and their reactions under long-wave UV (bottom). Photos by Ravenya Atchalak.

Raman analysis using 514 nm laser excitation on the "box bead" surfaces and outer nacreous layers of the sawn surfaces showed typical aragonite features at around 701/704 cm^{-1} (doublet) and 1085 cm^{-1}. The columnar radiating area on sample 2 was also analyzed, revealing features at around 154, 281, 711, and 1085 cm^{-1} that were consistent with calcite (J. Urmos et al., "Characterization of some biogenic carbonates with Raman spectroscopy," *American Mineralogist*, Vol. 76, 1991, pp. 641–646).

All the data obtained from the advanced testing methods as well as observation under magnification prove the "box bead" nuclei were fashioned from saltwater shell.

Although this is not the first time GIA has encountered saltwater cultured pearls containing non-traditional bead nuclei, the box shape of the beads in this sample group has never been documented in the gemological literature and is therefore notable.

Ravenya Atchalak
GIA, Bangkok

A type of multi-colored quartz with oriented inclusions, reportedly from Brazil. A special quartz called "Auralite 23" in the Chinese trade has recently appeared in the Donghai jewelry market in Jiangsu Province (figure 6). Sell-

Figure 6. Multi-colored quartz traded in the Donghai jewelry market in Jiangsu Province, China. Photo by Qingfeng Wu.

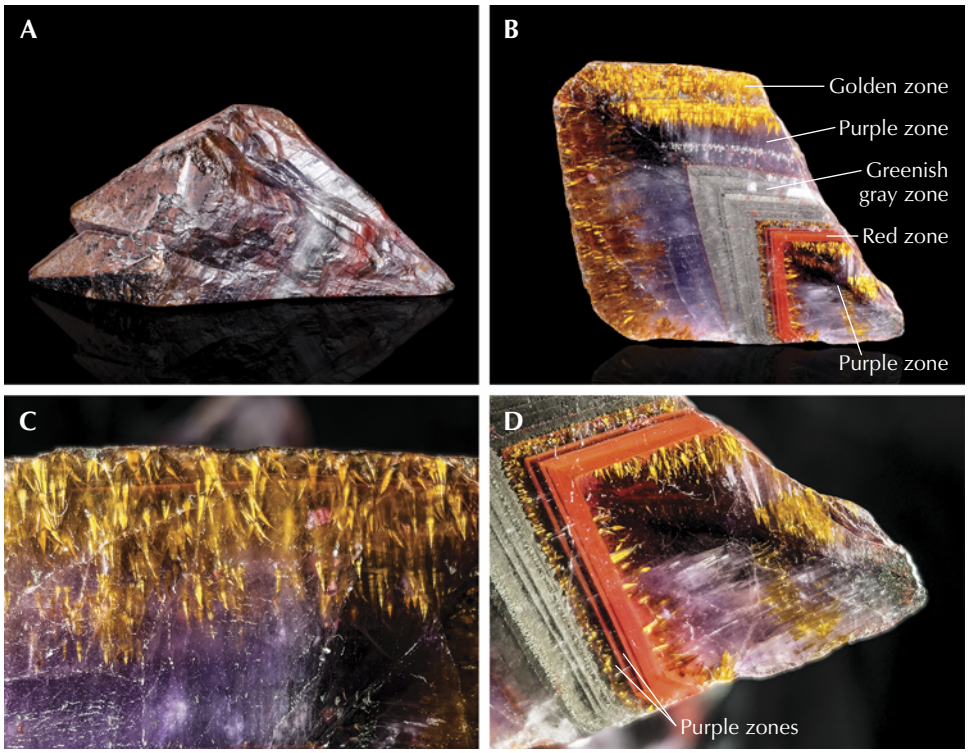

Figure 7. A: External characteristics of a piece of rough "Auralite 23" quartz measuring 8.2 × 5.5 × 3.7 cm. Well-developed rhombohedrons can be found on one side of the quartz, and the other side displays an uneven pyramidal shape with parallel striations. B: Five color zones and substantial oriented inclusions. C: Golden "broom-like" inclusions form a beautiful independent zone. D: Alternating purple and red zones. Photos by Zhuoxuan Li.

ers claim the material is from Brazil. The quartz is very similar to amethyst from Minas Gerais, Brazil (B.M. Laurs and N.D. Renfro, "Amethyst from Brazil with interesting inclusion patterns," *Journal of Gemmology*, Vol. 35, No. 6, 2017, pp. 468–469).

Four color zones (purple, red, greenish gray, and a second purple zone) are displayed when observed along the threefold axis. Sometimes, a separate golden zone can be formed (e.g., figure 7, B and C). The purple and greenish gray zones in the upper part of figure 7D are well defined, while the red and purple zones in the lower part show alternating growth bands. After cutting, substantial oriented inclusions can be found in each color zone. Golden "broom-like" inclusions observed in the purple zones are regularly distributed along the growth direction. Greenish gray horsetail-like inclusions are found in the middle of the quartz. In addition, red platelet inclusions appear in the red zone (figure 8). Notably, the platelet inclusions are seemingly restricted to this red zone and thus generate an agate-like zoning.

A multi-colored quartz slice was purchased and researched. The Fourier-transform infrared (FTIR) transmission spectra—with weak peaks at 3584 and 2331 cm^{-1}, medium strong peaks at 2924, 2850, 2671, 2597, 2498, and 2136 cm^{-1}, and strong peaks at 3454 and 2242 cm^{-1}—indicate that this is a natural quartz (figure 9).

Raman analysis identified the typical inclusions in the purple zones, with peaks at 246, 300, 387, 415, 550, and

Figure 8. Three representative solid inclusions in the multi-colored quartz. A golden "broom-like" inclusion in the purple region (A), greenish gray horsetail-like inclusions in the greenish gray region (B), and red platelet inclusions in the red region (C). Photomicrographs by Huizhen Huang; fields of view 1.35 mm, 0.6 mm, and 0.71 mm.

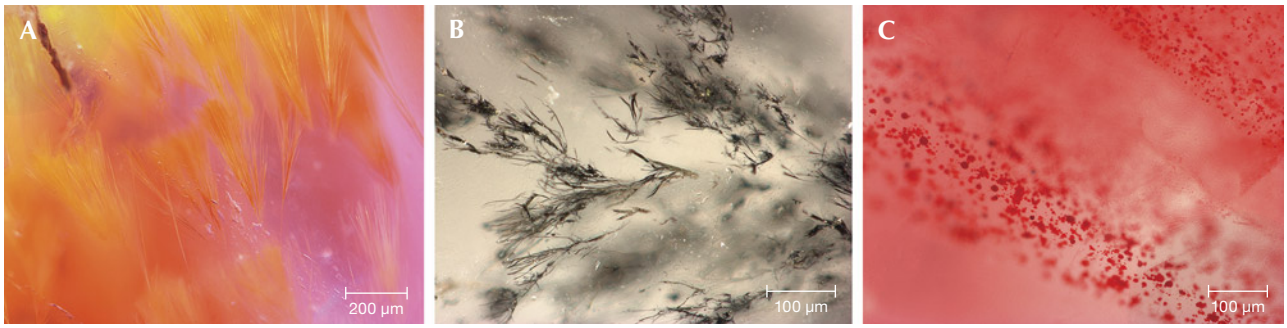

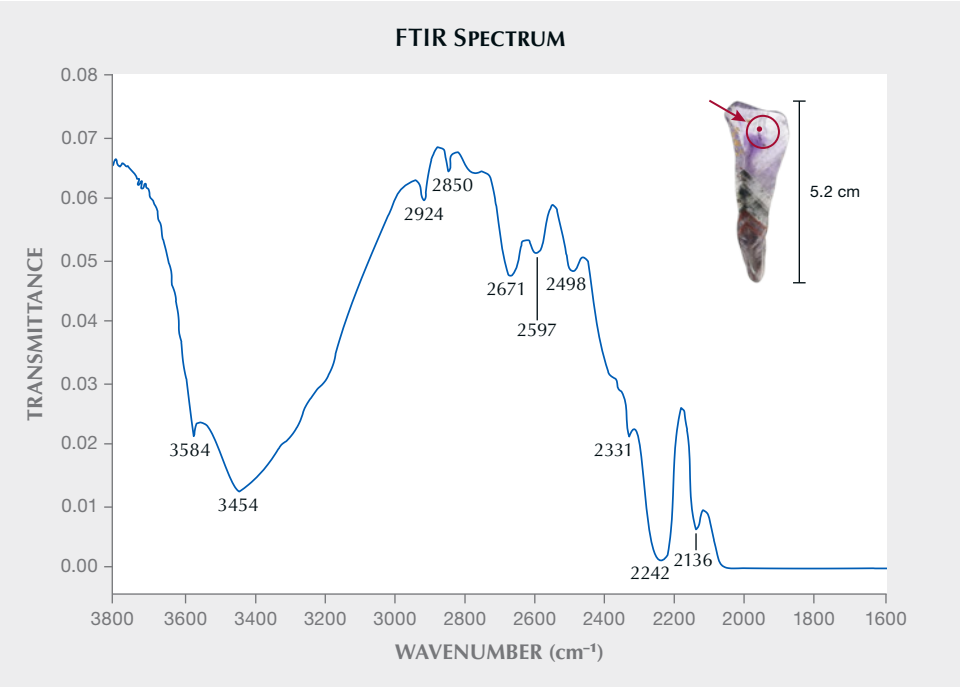

Figure 9. Fourier-transform infrared (FTIR) transmittance spectrum of the imaged quartz sample. A slice of the tested multi-colored quartz is shown in the inset.

685 cm^{-1} as goethite. The red platelet inclusions with peaks at 225, 245, 293, 411, 499, 611, and 1321 cm^{-1} are hematite (figure 10). The greenish gray horsetail-like inclusions could not be identified by Raman spectroscopy, so we carried out electron probe microanalysis (EPMA). The chemical analysis of these inclusions are mainly iron (45.49–46.51 wt.%) and sulfur (51.34–51.87 wt.%), indicating that they are FeS_2 inclusions.

Figure 10. Raman spectra of representative solid inclusions are shown along with the Raman reference spectra from the RRUFF database. Left: The purple zone contained a substantial amount of golden "broom-like" inclusions that matched with goethite. Right: The red platelet inclusions produced a Raman spectrum corresponding to hematite. The black numbers in this figure indicate the Raman peaks of the inclusion, and the gray numbers indicate the peaks of the quartz.

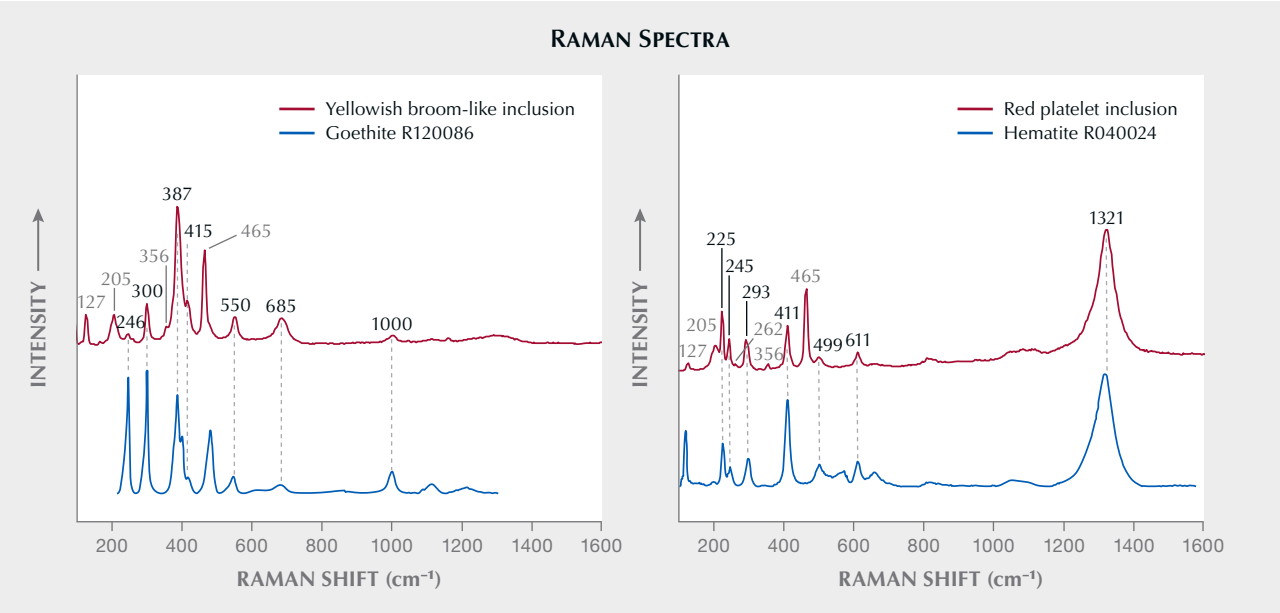

Considering the multi-colored zones and different oriented inclusions, this quartz likely formed and crystallized in multiple stages. However, the origin of this special pattern still remains unclear and is worth further research.

Huizhen Huang, Quanli Chen, and Yan Li
Gemmological Institute,
China University of Geosciences, Wuhan

Update from Mozambique's ruby mines. Mozambican rubies have revolutionized the dynamics of the ruby trade since their debut on the global gem scene in 2009. GIA has been following the evolution of the deposits around Montepuez in the Cabo Delgado Province of northern Mozambique since the very beginning (see W. Vertriest and S. Saeseaw, "A decade of ruby from Mozambique: A review," Summer 2019 *G&G*, pp. 162–183). In August 2022, a GIA field gemology team visited the mining area to document the current state of mining and to collect samples for future studies.

In less than a decade, the balance has shifted from an informal environment dominated by artisanal miners and foreign buyers to a situation that is mostly under the control of large-scale miners who bring these rubies directly to the global market.

There are currently three of these major operations working in the area east of Montepuez.

- Montepuez Ruby Mining (MRM): A partnership between Gemfields and local partner Mwiriti that has been mining rubies since 2012. Gemfields also mines Zambian emeralds at the Kagem mine.
- Fura Gems: This company has been involved in Mozambican ruby mining since 2019. Some of their concessions were previously worked by Mustang Resources. Fura is also actively mining Colombian emerald and Australian sapphire.
- GemRock: Owned by luxury jewelry brand DiaColor, this operation has been active on the ground since 2019.

In terms of geological formation, the ruby mineralization in the Montepuez area is not yet fully understood. The gems are generally described as amphibole-related corundum since the associated rocks are rich in amphibole. This mineral also dominates the inclusion scene of these gems.

While some primary mineralization is known and these ruby-bearing bodies are areas of interest for the mining companies, the rubies are seldom mined from the host rock. Nearly all of the mining activity is focused on the secondary deposits. These weathered gravel layers are rich in rubies and referred to locally as *camada*. This type of material is easy to mine, and the value of the ruby found here is higher than that in the primary deposits. The original host rock may contain higher volumes, but the majority of this corundum tends to be of very low grade. The exploration strategies of the mining companies focus heavily on identifying the extent, thickness, and distribution of the secondary gravels throughout their respective concessions. Understanding the geological formation of the corundum in this geological setting is a continuing process. Exploration teams are actively delineating and characterizing the ore bodies that hold the primary mineralization.

All three large-scale operations extract these ruby-rich gravels by stripping the overburden with excavators. This exposes the *camada*, which is dug up and stockpiled near the wash plants (figure 11). Local variations of the gravel

Figure 11. Mining of the gravels at Mugloto pit 3 in the MRM concession. The gravel layer is around 30 cm thick. The material on top has a distinct reddish tint that is typical for sediments in tropical environments. Under the layer of gravel, the weathered basement rock is more grayish in color. Photo by Wim Vertriest; courtesy of MRM.

Figure 12. The first step in the wash plant at Fura is the feeding bin (top left), where material enters the washing process. While the material moves down through the bins, water is added and a first screening removes large boulders. The trommel serves a dual function, breaking up clay lumps and screening out oversized materials. This image captures the first of seven steps to reduce the gravel to a concentrate rich in ruby, which is then handled in the sort house. Photo by Wim Vertriest; courtesy of Fura Gems.

layers can provide additional challenges. In some areas the sediment cover is less than 50 cm thick, which means the shallow gravel layer contains an abundance of roots, branches, and other organic material, making it harder to process further down the line. In other areas, the gravels are buried over 15 m deep, requiring serious effort and planning to strip the overburden. The ruby-rich layers themselves can vary from 10 to 150 cm; in some cases, multiple layers are present. The main one is always lying directly on the (extremely weathered) basement rock, which often consists of amphibolites, gneisses, and occasional felsic pegmatite veins.

While washing the rubies out of the gravel sounds very straightforward, this is a complex engineering process that requires careful monitoring and control. The gravels are unsorted, with quartz boulders up to 30 cm in diameter, but can also have a significant clay content. Processing them is no easy task and requires many steps of separating by size as well as various techniques to break up sediment clusters and concentrate the ore. Sizing is routine, but the other steps require considerable effort. At all of the large mining operations, logwashers, rotating trommels, and high-pressure water jets are used to break up clay clumps (figure 12). Concentration of the gravels (i.e., removal of the unwanted minerals) focuses on separating based on the specific gravities of the components of the sediment. Ruby is relatively dense compared to most other minerals such as feldspar and quartz. The most convenient method is using a pulsating jig where the waterlogged gravels move across a screen with barriers while getting pushed up vertically. This allows lighter materials to wash over the jig while denser minerals are concentrated at the bottom. While simple, this technique has its limitations, and several of the mines have progressed to more advanced techniques that allow for more precise separation and/or higher capacity, such as dense media separators and rotating pans in which a slurry with a precisely controlled density is used to separate heavier mineral fractions.

All of these techniques require large volumes of water. Plant operators assume that every metric ton of gravel processed requires 1000 liters of clear water. This water consumption was a decisive factor for development of the wash plant. For instance, a nearby river can serve as a cheap and constant supply of water, while boreholes are a much more costly alternative. As such, considerable effort is put into recycling water using settling ponds, cyclones, and flocculants. This allows much of the water, sometimes up to 90%, to be reused in the cleaning process.

With three large-scale mines operating in the area, the volumes of gravel processed are immense. The combined washing capacity of the three mines is more than 500 metric tons per hour.

The final product coming out of the wash plant is an intensely concentrated mix of heavy minerals enriched in ruby, though considerable portions of garnet, iron oxides, and other minerals are still present. Initially simple techniques such as manual sorting were used to handpick the rubies from this mix. As these operations grew, however, more advanced technology has been applied. Optical sorting devices are able to recognize rubies by their fluorescence and separate them from the mix. Most mines use these devices nowadays, often with manual control of the rejects since the machines are not flawless. In a final step, the mix of rubies is graded based on clarity, color, and size. Some mines perform this detailed and specialized task at company headquarters, while others do so at the mine. During the final stages of concentrating the rubies, security procedures become increasingly strict. Automatic sorting and gloveboxes (figure 13) are used to avoid contact with the rubies. The final grading, which must be done manu-

Figure 13. At GemRock, the concentrate from the wash plant is fed onto a conveyor belt where teams of sorters hand-pick the rubies. The workers are using glove-boxes to prevent physical access to the stones. At the end of the shift, the rubies are collected and inspected. Photo by Wim Vertriest; courtesy of GemRock.

ally by experienced specialists, is heavily supervised in secured spaces. This is one reason why some companies prefer to do this at their headquarters.

The further development and growing importance of these large-scale mining operations has also brought changes to the artisanal mining communities. These *garimpeiros* mined 100% of Mozambique's rubies in the first years after the discovery in 2009. Only in 2014 did the first rubies from large-scale mining reach the international market, through an auction hosted by MRM. Not all of these small-scale miners are local; many traveled from other provinces in Mozambique or even from neighboring countries such as Tanzania. In recent years, the importance of the *garimpeiro* in Mozambique's ruby market has been in decline. Legal codes were adjusted to make unlicensed mining a crime, allowing government officials to intervene with the artisanal mining activities that took place on the licenses of the large companies. As compensation, the government created *areas designadas* that were assigned to the artisanal miners. However, these are often small and nearly barren. At the moment, these areas cover an area of four square kilometers. The mining licenses secured by the large-scale mining companies cover over 2,000 square kilometers. Conflicts over mining rights have created considerable tension between established powers and the local communities. Some of these disputes are only now coming to light or are just beginning to be felt.

But the most drastic impact on the artisanal mining community has probably been the sanctions against the foreign buyers in the neighboring towns. Ruby buyers, mainly from Asia, have worked from offices near Montepuez to buy directly from the *garimpeiros* since 2008–2009, but their numbers have been drastically reduced in recent years. This has almost completely eliminated the main clientele for the artisanal ruby miners. During GIA's visit in 2016, huge numbers of *garimpeiros* (tens of thousands of them) could be seen working and traveling throughout all the mining concessions east of Montepuez. During GIA's recent 10-day expedition in August 2022, only 37 artisanal miners were seen in the same area. Most of the artisanal activity has moved farther east toward the city of Chiure, where the *garimpeiros* are mining more recent river sediments that are rich in rubies. Many have returned to their home villages, while some of the locals have found employment with the large mining companies.

The Cabo Delgado Province is currently experiencing social and political turmoil. Religious extremist groups under the name Ahlu-Sunna wa al Jama'a have been growing more violent. This has forced many people to abandon their villages and relocate to the southern reaches of the provinces, where the mines are located. One company reported that the number of people residing on their mining license increased from 1,500 to more than 20,000 in less than one year.

The local political structure also lacks the strength to successfully empower the local communities. All large-scale miners pay significant royalties and taxes to Mozambique's central government. Unfortunately, many of these funds fail to reach the historically underprivileged communities surrounding the mines in the northern Cabo Delgado Province. This only amplifies social unrest. Many local projects have been set up by the large companies as part of their own corporate social responsibility programs, focusing on a sustainable food supply, transportation, and healthcare.

The last five years have brought dramatic change to ruby mining around Montepuez. Nowadays the dominant players are the larger operations and no longer the *garimpeiro* community with their associated trading network. These large-scale miners have immensely upgraded and professionalized

Figure 14. This bracelet containing 12 mm beads was submitted as "root amber." Photo by Tsung-Ying Yang.

their operations since their initial exploration and early mining phases. They have integrated more sophisticated techniques in both the gravel processing and the sorting. Larger fleets of machinery and fine-tuned wash plants allow huge volumes of ruby ore to be handled. This has resulted in a more stable ruby supply to the international markets.

However, the situation on the ground remains unstable, with social unrest growing in the wider areas where the ruby mining is happening. Only time will tell how this situation will evolve.

Wim Vertriest and Sudarat Saeseaw
GIA, Bangkok

Kevin Schumacher
GIA, Carlsbad

SYNTHETICS AND SIMULANTS

Pressed amber imitation of "root amber." Root amber, a commercial variety of burmite (amber from northern Myanmar), is popular in the Taiwanese market. As the name suggests, root amber resembles tree roots and usually has a dark brown to light yellow color with creamy swirls caused by the mixing of fine calcite particles and resin during the sedimentation of the amber (Y. Wang, *Amber Gemology*, China University of Geosciences Press, Beijing, 2018, p. 244).

Recently, a bracelet was submitted to Taiwan Union Lab of Gem Research (TULAB) as root amber (figure 14). This bracelet consisted of a string of dark brown beads with light yellow creamy swirls. The refractive index of these beads was about 1.54 by spot reading, which was consistent with the RI of amber, and the beads showed uneven medium blue to faint yellow fluorescence under long-wave UV light. Microscopic observation of the beads revealed slight differences from natural root amber. First, the yellow swirls appeared to have a coarse texture rather than smooth. Second, the brown regions seemed to show a vaguely granular structure. The beads were further investigated under a microscope with long-wave UV illumination and compared with those of natural root amber. The results of fluorescence microscopy revealed that these regions did, in fact, show a granular structure with particle sizes ranging from tens to hundreds of microns, while the natural root amber appeared relatively fine-grained and homogeneous under the same lighting (figure 15). Raman spectroscopic analysis and comparison with both the

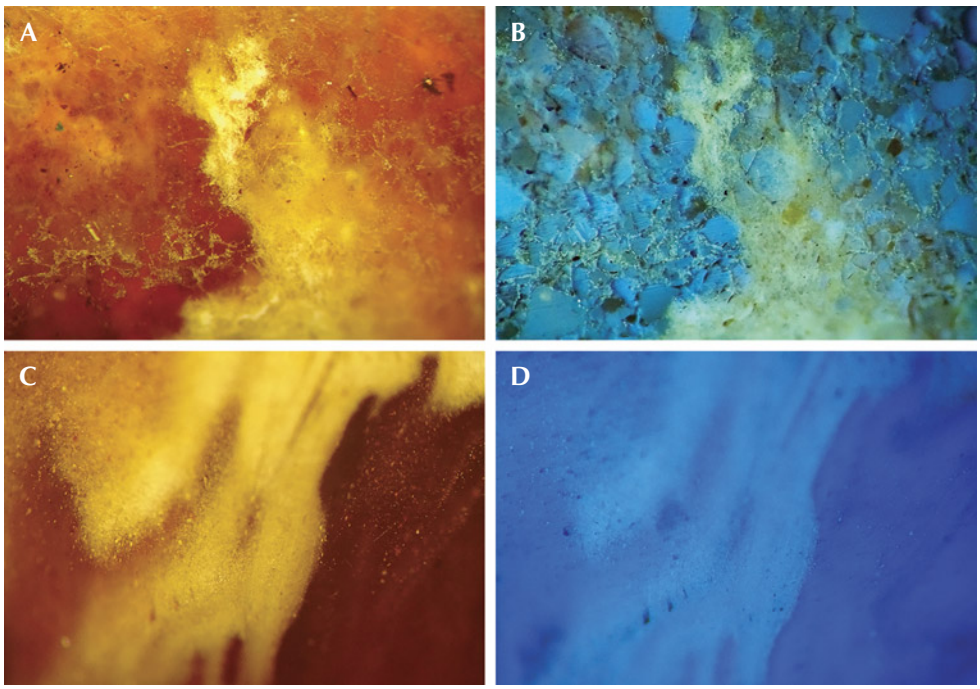

Figure 15. Pressed amber imitations and natural root amber. Under white light, the pressed amber (A) appeared less homogeneous than natural root amber (C). Granular structure of the pressed amber (B) revealed under long-wave ultraviolet light, whereas natural root amber showed relatively even fluorescence (D) under the same long-wave UV lighting. Photomicrographs by Kai-Yun Huang; field of view 4.23 mm.

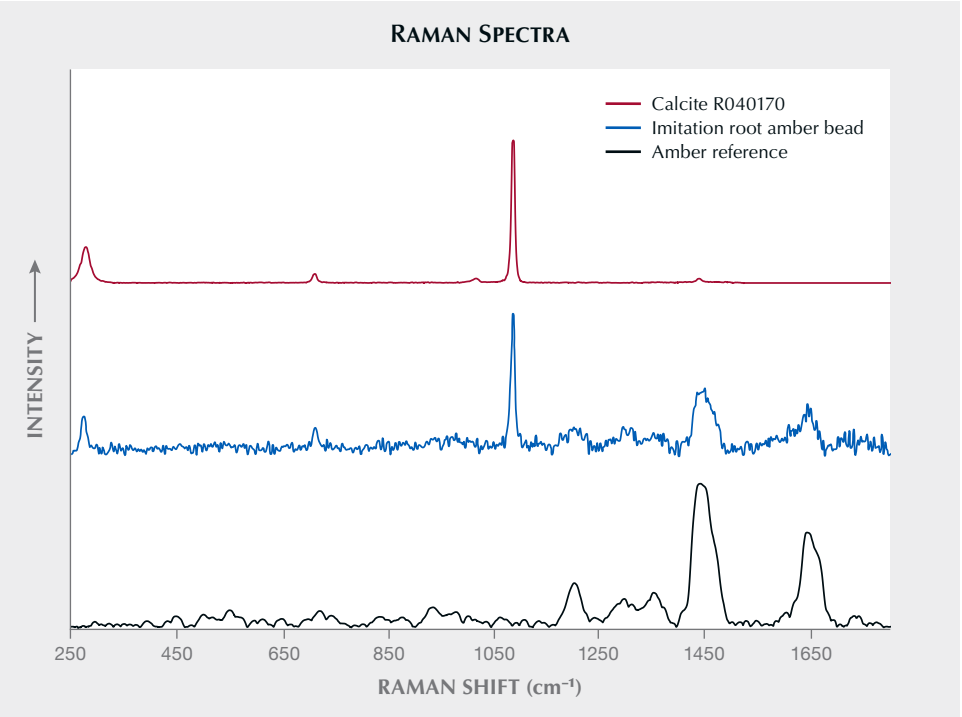

Figure 16. Raman spectra comparisons between the spectrum of the bead, amber reference (TULAB), and that of calcite from the RRUFF database suggested that the bead consisted of calcite and amber. The peaks at 1645 and 1450 cm^{-1} may be assigned respectively to ν(C=C) and δ(CH_2) modes in fossil resin. The stacked spectra are baseline-corrected and normalized.

RRUFF database and the internal amber references compiled by TULAB confirmed that these beads were made of amber and calcite particles (figure 16). Previous studies also pointed out that the strongest peaks at 1645 and 1450 cm^{-1} may respectively be assigned to ν(C=C) and δ(CH_2) modes in fossil resin (R.H. Brody et al., "A study of amber and copal samples using FT-Raman spectroscopy," *Spectrochimica Acta Part A*, Vol. 57, No. 6, 2001, pp. 1325–1338). To summarize, the amber bracelet should be defined as an imitation—specifically, a pressed amber mixed with calcite powder during the manufacturing process.

Although pressed amber has long existed in the trade, the addition of calcite powder made this sample a better imitation of natural root amber and more difficult to distinguish by standard gemological testing. The best identification method for such an imitation is observation with fluorescence microscopy.

Shu-Hong Lin
Institute of Earth Sciences,
National Taiwan Ocean University
Taiwan Union Lab of Gem Research, Taipei

Tsung-Ying Yang, Kai-Yun Huang, and Yu-Shan Chou
Taiwan Union Lab of Gem Research, Taipei

Synthetic sapphire with Rose channels. The Laboratoire Français de Gemmologie (LFG) received a 15.84 ct light purplish blue corundum for identification (figure 17). Under the microscope, clouds of bubbles similar to those seen in synthetic corundum were observed (figure 18), along with twinning planes and hollow channels known as Rose channels (figures 18 and 19). The Rose channels, which are always found at the intersection of twin lamellae, were crystallographically oriented along the edges of the rhombohedral faces and formed angles of about 90° (again, see figure 18); these features are normally seen in natural corundum (F. Notari et al., "'Boehmite needles' in corundum are Rose channels," Fall 2018 *G&G*, p. 257).

Rose channels and twinning lamellae are common in natural corundum but seldom reported in synthetic corundum, including one instance in a Ramaura flux synthetic ruby (E. Fritsch et al., "Are boehmite needles in corundum Rose channels?" *Geophysical Research Abstracts*, Vol. 20, EGU2018-19493, 2018). This is because the twinning

Figure 17. A 15.84 ct light purplish blue synthetic sapphire measuring 15.35 × 14.05 × 8.25 mm. Photo by U. Hennebois.

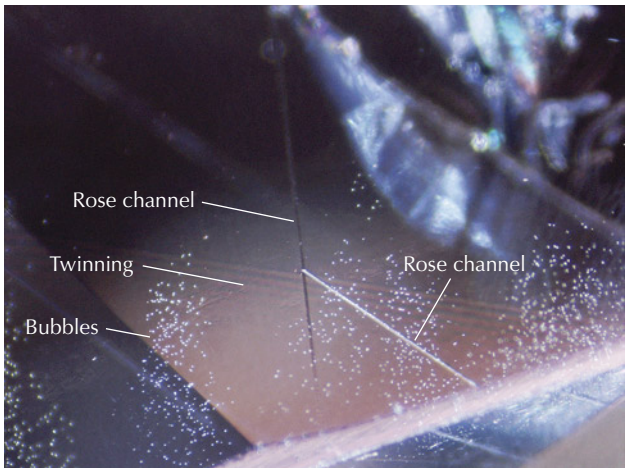

Figure 18. Clouds of bubbles, Rose channels, and twinning planes in the synthetic corundum under crossed polarizers. Photomicrograph by U. Hennebois; field of view 3 mm.

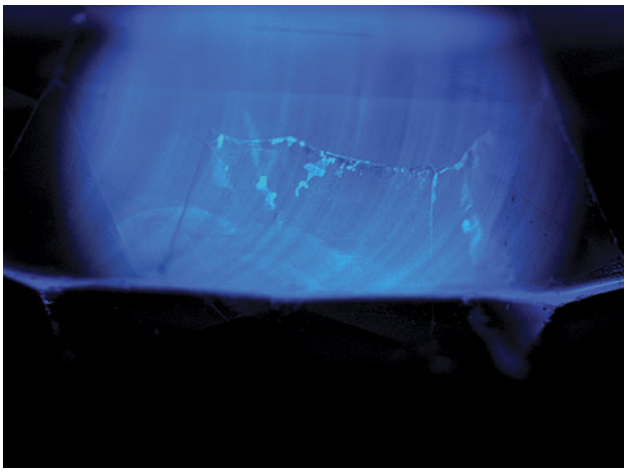

Figure 20. DiamondView imaging revealed curved growth lines characteristic of synthetic Verneuil corundum. Image by A. Herreweghe; field of view 10 mm.

lamellae is most often formed via deformation twinning and results from post-growth events; thus, it is frequently observed in natural samples.

The sample was inert under long-wave UV and presented strong blue luminescence under short-wave UV. No gallium was detected with energy dispersive X-ray fluorescence, which further confirms that this corundum was synthetic (S. Muhlmeister et al., "Separating natural and synthetic rubies on the basis of trace-element chemistry," Summer 1998 *G&G*, pp. 80–101). DiamondView imaging showed curved growth lines, characteristic of Verneuil flame-fusion synthetic corundum (figure 20). Rose channels in corundum were linked in the past with boehmite needles and the characteristic absorptions in the 1500–4000 cm^{-1} region (Notari et al., 2018); however, no absorptions were observed in this region of the FTIR spectrum.

Although by far most common in natural corundum, the presence of Rose channels and twinning planes in synthetic corundum serves as evidence that these features alone cannot be used to confirm natural origin.

Ugo Hennebois, Aurélien Delaunay, Annabelle Herreweghe, and Stefanos Karampelas (s.karampelas@lfg.paris)
LFG, Paris

Emmanuel Fritsch
University of Nantes, CNRS-IMN, France

Figure 19. Clouds of bubbles, Rose channels, and twinning planes in the synthetic corundum. Photomicrograph by U. Hennebois; field of view 10 mm.

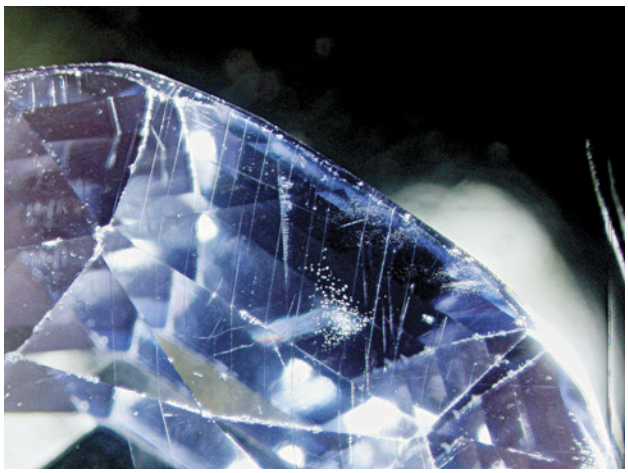

TREATMENTS

Gemological characteristics of low-temperature "gel-filled" turquoise. In the past decade, low-temperature "gel-filled" turquoise (X. Yating and Y. Mingxing, "Filling material and characteristic of polymer-impregnated turquoise in Anhui Province," *Journal of Gems and Gemmology*, Vol. 21, No. 1, 2019, pp. 20–30) has been sold in the Chinese market. This special gel filling treatment is quite different from previous resin-filling or impregnation treatments (L. Liu et al., "Technical evolution and identification of resin-filled turquoise," Spring 2021 *G&G*, pp. 22–35). The rough turquoise materials are soaked in a polymer composite gel at –10° to –15°C (without pressure) for filling and enhancement of appearance. According to the information obtained from a turquoise factory in Shiyan city, Hubei Province, the process can be generally summarized as follows:

1. The rough turquoise material is selected, cut, washed, and dried at about 100°C.
2. The material is immersed in a polymer composite

Figure 21. Untreated rough turquoise material produced in Zhushan County, Hubei Province, China, including one piece (indicated with the dotted line) that was selected to be cut into several square pieces. Photo by Andi Zhao.

gel solution, then put in the refrigerator and soaked at –10° to –15°C for 7–10 days.

3. The turquoise material is removed from the refrigerator and heated from room temperature to 80° at 1°C/min, followed by soaking at 80°C for four hours.
4. The material is further heated by ramping the temperature from 80° to 120°C at 1°C/min, followed by soaking at 120°C for eight to ten hours.
5. The turquoise material is then cooled from 120°C to room temperature at 3°C/min.
6. After removal from the furnace, the gel residue is removed by polishing off the surface layer.

The authors selected a piece of rough turquoise material (figure 21) produced in Zhushan County in Hubei Province, China, and cut it into several square pieces. According to the above treatment process, the turquoise was filled using the gel solution provided by the turquoise factory in Hubei. The material before treatment (N-1) was light whitish blue, with uneven color distribution, and black impurities were locally distributed. After treatment, the material's color deepened to a more desirable blue-green and became more uniform (figure 22), still retaining the original black impurities. After polishing, the surface of the gel-filled turquoise had a waxy luster and the hydrostatic specific gravity changed from approximately 2.32 to 2.21 due to the lower SG of the

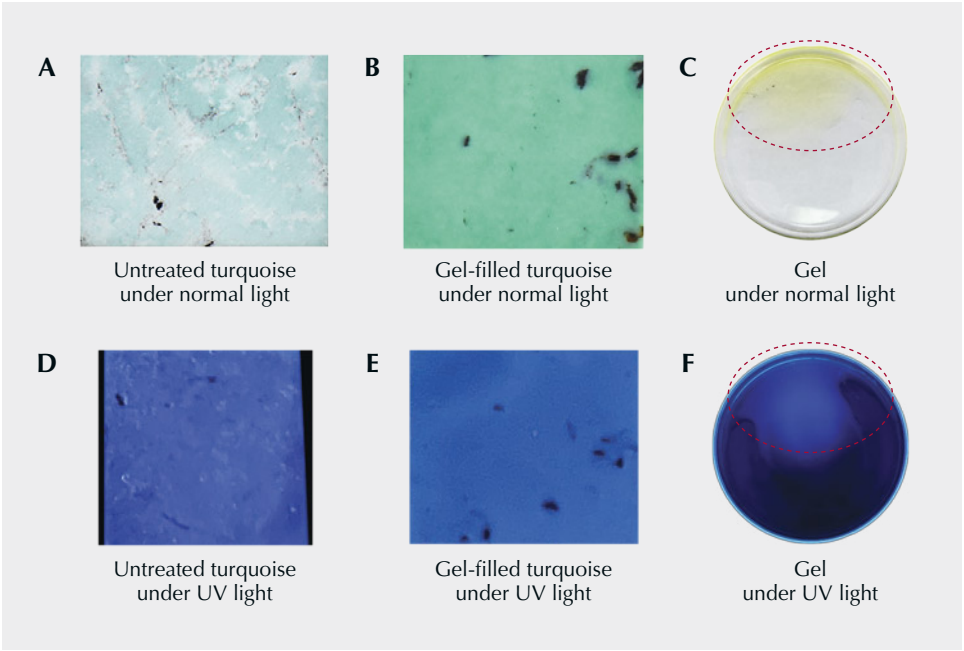

Figure 22. These images show the untreated turquoise, the gel-filled turquoise, and the gel solution in glassware under normal light (A–C) and under UV light (D–F). Photos by Andi Zhao.

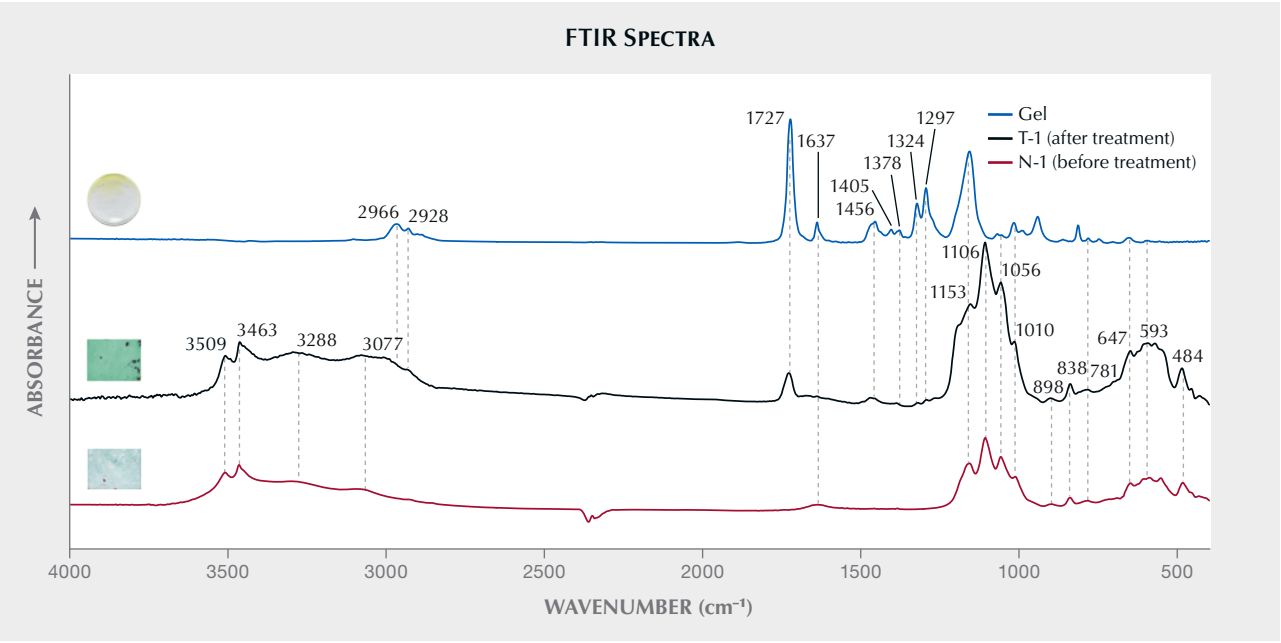

Figure 23. FTIR spectra of the gel, untreated turquoise, and low-temperature gel-filled turquoise. The characteristic peaks for gel-filled turquoise are a series of peaks at 2966, 2928, 1727, 1637, 1456, 1405, 1378, 1324, and 1297 cm^{-1} that are caused by the gel.

gel (approximately 1.00). The turquoise before treatment showed medium-light bluish white fluorescence with an abundance of white spots. After treatment, it showed uniform medium bluish white fluorescence (figure 22) under long-wave UV fluorescence. The turquoise was inert to short-wave UV before and after treatment. The light yellow gel solution showed a strong bluish white fluorescence along the edge of the glassware under long-wave UV and was inert under short-wave UV.

Fourier-transform infrared (FTIR) spectra of the gel and turquoise samples (before and after treatment) are shown in figure 23. Typical peaks for turquoise were observed, namely two absorption peaks at 3509 and 3463 cm^{-1} caused by the stretching vibration of hydroxyls (OH) (Q. Chen et al., "Turquoise from Zhushan County, Hubei Province, China," Fall 2012 *G&G*, pp. 198–204). Due to strong hydrogen bonding associated with the hydroxyl groups, the absorption peaks are relatively sharp. The absorption peaks at 3288 and 3077 cm^{-1} caused by OH stretching of water molecules are relatively flat, while the peak associated with the bending vibration of water is near 1637 cm^{-1} and the intensity of the absorption peak is relatively weak. There are four absorption peaks produced by the PO_4 stretching vibration between 1000 and 1200 cm^{-1}, which appear near 1153, 1006, 1056, and 1010 cm^{-1}. In addition, the gel-filled turquoise showed a weak absorption peak (2928 cm^{-1}) caused by a CH_2 stretching vibration and a strong stretching vibration peak (1727 cm^{-1}) caused by C=O (Yating and Mingxing, 2019). A series of weak small absorption peaks also appeared at 1456, 1324, and 1297 cm^{-1}. These spectral peaks are consistent with the FTIR spectra of the gel. The spectral peaks can also be used to distinguish between untreated and gel-filled turquoise. Gas chromotography–mass spectrometry identified the main components of the gel as methyl isocrotonate ($C_5H_8O_2$, 46.05 wt.%), cyclooctatetraene (C_8H_8, 35.8 wt.%), and oxirane (C_2H_4O, 5.93 wt.%).

Quanli Chen
Gemmological Institute,
China University of Geosciences, Wuhan
School of Jewelry, West Yunnan University of
Applied Sciences, Tengchong

Andi Zhao, Yan Li, Yanhan Wu, and Tianchang Liu
Gemmological Institute,
China University of Geosciences, Wuhan

CONFERENCE REPORTS

Inaugural Turquoise United conference. The first-ever Turquoise United conference was held August 11–13, 2022, in Albuquerque, New Mexico. This multifaceted event was organized and hosted by Joe Dan Lowry and his son Jacob, part of a fifth-generation family in the turquoise industry. All activities took place in the Turquoise Museum (www.turquoisemuseum.com), owned and operated by the family and the Albuquerque Convention Center (figure 24).

Turquoise has been treasured and used by many different cultures for thousands of years. As an aggregate gem-

Figure 24. Left: The entrance to the Turquoise Museum. Photo by Jacob Lowry/Turquoise Museum. Right: A corner in the origin display room shows rough and polished samples from Tyrone and Cerrillos, two well-known deposits in New Mexico. Photo by Tao Hsu.

stone, it also poses a challenge for traders. Possibly more so than for any other gemstone, the buying, selling, and owning of a turquoise piece can be an intensely personalized experience. A combination of factors including color, matrix pattern, specific mine origin, and the presence or absence of treatment come into play, making each piece unique. Turquoise United provides a platform for everyone involved in the trade to gather as a community and discuss important topics. About 100 delegates from different countries attended the inaugural event, including miners, cutters, treatment experts, dealers, television shopping network suppliers, collectors, jewelry designers, enthusiasts, consumers, appraisers, and scientists. GIA sent research and education representatives to connect with the turquoise community and learn from the experts. We had the opportunity to interview over 10 industry experts, including members of the domestic and international trade, miners, and artisans involved in turquoise treatment and the manufacture of imitation turquoise (figure 25). The content gathered will be highlighted in future GIA educational programs.

A wide variety of activities made this educational conference enjoyable. An evening gala and auction kicked off

Figure 25. Russell Twiford III holds a massive resin imitation of turquoise he created, which is now displayed at the Turquoise Museum. Photo by Aaron Palke.


Figure 26. Left: Attendees enjoy a conversation about Southwestern-style jewelry design and manufacture outside the Turquoise Museum. Right: Joe Dan Lowry and son Jacob were the auctioneers at the kickoff gala. Photos by Tao Hsu.

the event (figure 26). Auction items included finished turquoise pieces, specimen and finished stone sets, and a bracelet featuring more than 200 inlay pieces designed and donated by GL Miller (Studio GL, Albuquerque). All other items were provided by the museum, and the proceeds will be allocated for future Turquoise United events. Delegates had the opportunity to view representative items from domestic and international sources such as Yungaisi, China (figure 27). All items were auctioned by the end of the gala. Each attendee received a gift bag containing a piece of turquoise, including some nice cabochons.

During the day sessions, experts including Joe Dan Lowry, GL Miller, and author AP hosted identification panels at the Turquoise Museum (figure 28). Panelists evaluated the identity and origin of various turquoise jewelry pieces submitted by participants. The panel attracted consumers and enthusiasts who shared the stories behind their treasures. In the turquoise collector community, mine origin is an extremely important aspect. Turquoise enthusiasts often spend a lifetime putting together a collection of quality pieces from the most important turquoise mines, especially from the American Southwest. Lowry and

Figure 27. A 9.32 ct backed turquoise from Yungaisi, China, purchased during the auction at the Turquoise United conference. Photo by Aaron Palke.

Figure 28. Turquoise enthusiasts and consumers brought their jewelry pieces to the identification panel experts, who shared their opinions on the pieces and answered questions from the audience. Photo by Tao Hsu.

Figure 29. Top: Joe Dan Lowry proposes a turquoise grading system alongside a panel of experts. Photo by Tao Hsu. Bottom: A look at the color scale and master stones for blue turquoise included in Lowry's grading system. Photo by Joe Dan Lowry.

Miller impressed the audience with their knowledge of historic turquoise mine characteristics, and engaged in much discussion about the complexity involved in conclusive identification and origin determination.

Two evening discussion panels took place in the Albuquerque Convention Center, with one focused on the vision and educational function of Turquoise United and the other on turquoise grading. The authors participated in both panels along with delegates from all aspects of the industry. Author TH noted the current lack of turquoise-related educational programs and the potential industry benefit of reaching a broader audience not limited just to turquoise traders.

The second panel centered on Joe Dan Lowry's proposal for a turquoise grading system that could be applied inside and outside of the turquoise community (figure 29). Lowry's grading system is based on an unsurpassed collection of turquoise master stones of various qualities from global sources accumulated by the Lowrys over five generations. In the proposed grading system, origin is considered separately from other quality factors. A scoring system is based on a scale of 0 to 100, with the most important factor being color (70% of the final score) and additional consideration given to the aesthetics of the matrix (20%) as well as "zat" (10%), a combined description of the dynamic and boldness of both the color and the matrix patterns. Different levels of "zat" can be described as dynamic and bold in contrast to dull, flat, or uninteresting. After the quality evaluation and considering the importance of origin in many cases, the result would be combined with the condition of the piece (treated or untreated), cut, weight, and backing to give the buyer a complete picture of the stone. The panelists had a lengthy discussion on the applicability of the grading system, and author AP shared his views on consistency and potential market impact with the attendees.

In addition to the educational activities, a small-scale turquoise show took place in the courtyard of the museum. A dozen dealers participated, displaying rough and finished turquoise to attendees (figure 30). To keep the event focused, dealers could only sell turquoise stones and not finished jewelry. Turquoise from the southwestern United States, Mexico, China, and Iran were all featured at the show.

Figure 30. Left: A turquoise show attendee checks out polished pieces from multiple southwestern U.S. deposits. Photo by Tao Hsu. Right: An assortment of high-quality natural Persian turquoise cabochons; the one being held weighs about 19 ct. Photo by Aaron Palke.

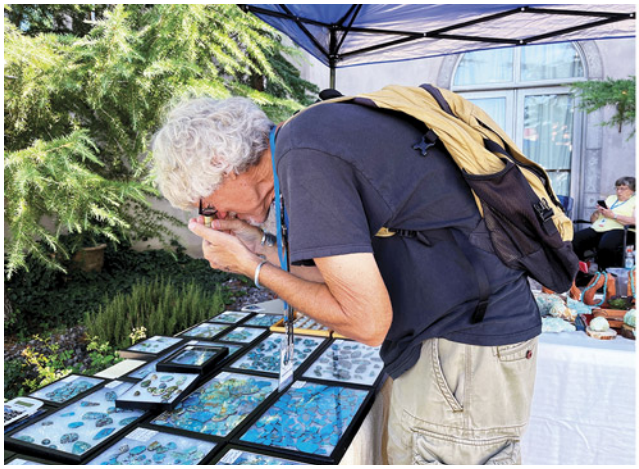

Figure 31. The historic Tiffany mine in the Cerrillos mining district. This pit was mined many hundreds of years ago by Native Americans before contact with European cultures. Photos by Aaron Palke.

Surrounded by historic turquoise mines (figure 31) and Native American communities that have contributed enormously to the popularity of turquoise in the United States through their iconic turquoise jewelry designs, Albuquerque was the perfect setting for the conference. The annual Santa Fe Indian Market (SFIM), held every August, is also in close proximity. This year marks the hundredth anniversary of this famous event celebrating Native American arts and fashion, which features turquoise and turquoise jewelry. While the second Turquoise United conference is set for Albuquerque, the Lowrys are already planning future events and considering other important turquoise centers to host the conference as well.

Tao Hsu and Aaron Palke
GIA, Carlsbad

ANNOUNCEMENTS

Ahmadjan Abduriyim receives JAMS award for applied mineralogy. The Japan Association of Mineralogical Sciences (JAMS) has named Dr. Ahmadjan Abduriyim as the recipient of its 2021 award for applied mineralogy (figure 32). As president of Tokyo Gem Science and director of GSTV Gemological Laboratory in Tokyo, Abduriyim was recognized for his contributions to applied mineralogy.

Abduriyim holds a PhD in mineralogy and geology from Kyoto University and is a former senior manager and senior scientist at GIA's Tokyo laboratory. A longtime *G&G* contributor and editorial review board member, Abduriyim has published numerous articles on topics related to diamonds, colored stones, and organic gem materials in various journals, including *G&G*, *Journal of Gemmology*, and *Australian Gemmologist*.

Abduriyim's research has covered geographic origin determination of major gemstones, advanced testing of colored stones, and the application of laser ablation–in-

Figure 32. Dr. Ahmadjan Abduriyim (left) receives the 2021 Japan Association of Mineralogical Sciences (JAMS) award for applied mineralogy.

Figure 33. A view of the GSTV Gem Museum in Tokyo, exhibiting the extensive gem and mineral collection of the late Akira Chikayama. Photo by Ahmadjan Abduriyim.

ductively coupled plasma–mass spectrometry (LA-ICP-MS) in the gemological field. Most recently, Abduriyim has worked to integrate information obtained from the following three areas of research: the collection of geological data and gem samples from field surveys of mines worldwide, the application of high-precision analytical methods, and the construction of a database for the latest geographic origin determination and individual identification. He and his team are currently researching the usefulness of LA-ICP-MS in measuring trace elements and U-Pb isotope dating for geographic origin determination.

Meanwhile, Abduriyim recently honored Akira Chikayama, Japan's "Father of Gemology," by opening a museum featuring Chikayama's collection of rocks, minerals, and gemstones at GSTV Gemological Laboratory (figure 33). Chikayama, an esteemed gemology instructor, collected rock, mineral, and gemstone samples from international mines and trade shows for use in his courses, eventually amassing a collection of more than 30,000 specimens. After his passing in 2007, the collection went unused until Abduriyim had the opportunity to view it in 2016 and envisioned creating a museum to share the collection with the world. In May 2022, the GSTV Gem Museum opened, displaying Chikayama's vast collection as well as several hundred books and magazines. On display are more than 600 rock specimens, 2,000 mineral specimens, 25,000 rough gemstones/gemstones in matrix (figure 34), 500 transparent crystals, 2,500 faceted stones, and 300 synthetic and imitation stones. The museum is not only an exhibition of Chikayama's collection, but also a place for visitors to learn about the fascinating world of gemology.

Erica Zaidman
GIA, Carlsbad

Figure 34. A portion of Chikayama's crystal specimens featured in the GSTV Gem Museum. Photo by Ahmadjan Abduriyim.

Figure 35. A gem pocket replica highlighting various gems and minerals mined in San Diego County, including tourmaline, quartz, kunzite, aquamarine, and mica. Dubbed the "Miner's Fantasy Mine," this replica combines various gems and minerals in the same pocket for illustrative purposes only. Photo courtesy of the San Diego Natural History Museum.

***Hidden Gems* at the San Diego Natural History Museum.** Known locally as The Nat, the San Diego Natural History Museum is making good use of unoccupied space with its *Hidden Gems* exhibit. Spanning the five floors of the museum, the 2,000 square foot vertical gem and mineral exhibit fills the space outside of the elevators on each floor, providing a permanent home to more than 100 specimens from the museum's collection, many of which had not been on display prior to the exhibit's opening. In this vertical exploration, visitors can expect to be wowed with a different experience as they reach each level of the museum.

Each floor has its own theme designed to showcase the diversity of minerals from all over the world. Fluorescent minerals are aglow under black lights on the lower level.

Figure 36. An image of quartz agate from Chihuahua, Mexico, scanned from the specimen and used to create wallpaper featured on Level 4 of the museum. Photo courtesy of the San Diego Natural History Museum.

Level 1 displays a sampling of gems from all over the world, with a special case dedicated to birthstones from GIA. Level 2 is comprised entirely of gems mined locally in San Diego County, California, including quartz, topaz, and hot pink tourmaline. This level also features a replica gem pocket full of gemstones found in the area (figure 35). Level 3 focuses on the application of minerals in the real world, including a section highlighting the minerals used to make cell phones. Finally, Level 4 covers geologic diversity, presenting a wide array of gems and minerals of different colors, shapes, and sizes. After experiencing all five floors, visitors leave with an understanding of the many roles of gems and minerals—aesthetic, geological, and practical.

The walls and ceilings of the exhibit also deserve honorable mention. Large-scale murals produced by scanning various mineral specimens and printing them on the wallpaper create the feeling of walking into the featured mineral (figure 36). And a 24-foot sculpture modeled after the crystalline structure of silicate dangles from the ceiling.

Hidden Gems is a long-term exhibit and will occupy the space outside the elevators for the near future, until the museum unveils another innovative exhibit to fascinate visitors. For now, *Hidden Gems* is a vertical delight for all to see. Visit https://www.sdnhm.org/exhibitions/hidden-gems/ to learn more.

Erica Zaidman

***The Year of Mineralogy* at the Perot Museum.** 2022 is the International Mineralogical Association's designated year for celebrating the history, development, and role of mineralogy, with a goal of promoting public interest in mineral studies. The association aims to emphasize mineralogy's critical role in technology and society and to highlight the future of mineralogy through the exploration of new and environmentally

Figure 37. The Year of Mineralogy *at the Perot Museum of Nature and Science in Dallas features 10 cases filled with fascinating samples demonstrating the importance of the mineral world around us. Photo courtesy of the Perot Museum of Nature and Science.*

conscious methods for extracting the minerals used today. To help carry out this mission, the Perot Museum of Nature and Science in Dallas has created the *Year of Mineralogy* exhibit (figure 37) in the Lyda Hill Gems and Minerals Hall (https://www.perotmuseum.org/exhibits/halls/lyda-hill-gems-and-minerals-hall/).

With more than 5,700 minerals identified to date, and more added each year, there is no shortage of specimens to display. Each of the exhibit's 10 cases educates visitors with spectacular examples to illustrate various mineral properties. The first case defines what a mineral is, showing specimens such as lapis lazuli and lazurite (figure 38). Chemical composition and crystal structure are explained in the second case, while the remainder are dedicated to the various properties of minerals, including hardness, tenacity, streak, luster (figure 39), and color.

"By understanding mineral characteristics, like hardness, magnetism, and specific gravity, we are able to find

Figure 38. This striking example of lapis lazuli, a rock composed of minerals including lazurite, pyrite, and calcite, is on display in the exhibit. From the Sar-e-Sang mine in the Kokcha River area of Badakhshan Province, Afghanistan. Photo courtesy of the Perot Museum of Nature and Science; specimen courtesy of Keith and Diane Brownlee.

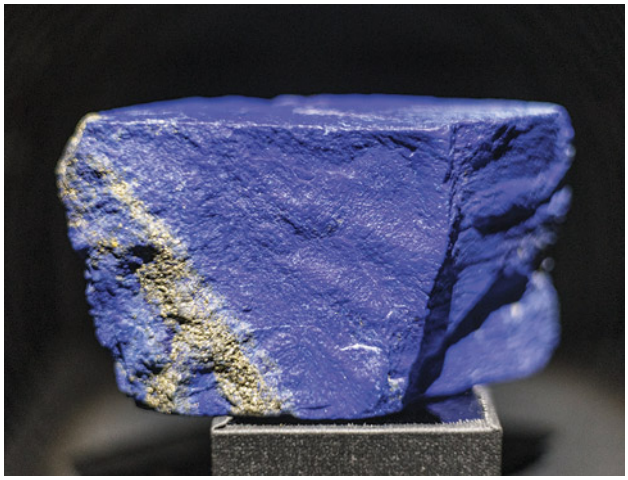

Figure 39. The resinous appearance of this sphalerite specimen highlights the mineral property of luster. From the Picos de Europa Mountains, Asturias, Spain. Photo courtesy of the Perot Museum of Nature and Science; specimen courtesy of Gail and Jim Spann.

solutions to many modern industrial problems and improve our overall well-being," said Kimberly Vagner, director of gems and minerals at the Perot Museum.

On display until April 24, 2023, the exhibit is an opportunity for all ages to acquire a deeper understanding of the mineral world around us. Can't make it to Dallas before April 24? Follow the museum's Lyda Hill Gems and Minerals Hall on Instagram for posts highlighting some of the magnificent minerals on display.

Erica Zaidman

IN MEMORIAM

Andrew Cody. Australian opal leader Andrew Cody (figure 40) passed away on September 12, 2022, at the age of 71. Internationally regarded as one of Australia's foremost opal wholesalers, cutters, and exporters, Cody was instrumental in the establishment of opal as Australia's national gemstone and the development of standard opal nomenclature.

Collecting fossils, gemstones, and minerals since the age of 12, Cody began cutting opal in 1964 after a class trip to the famous deposit at Coober Pedy. In 1971, at the age of 20, he established Cody Opal, a wholesale opal and gem cutting business, which later began exporting worldwide. Cody was the joint founder of the National Opal Collection, an Australian opal and opal jewelry supplier with showrooms and museums located in Sydney and Melbourne.

Over the course of his career, Cody served in a number of leadership positions, including president of the Australian Gem Industry Association and president of the International Colored Gemstone Association. He was awarded honorary fellowships from the Australian Gemmological Association and the Gemmological Association of Great Britain. Also an author, Cody published two books. *Australian Precious Opal – A Guide Book for Professionals* (1991) was followed by *The Opal Story: A Guidebook* (2010), written with his brother Damien and published in six languages.

Figure 40. Andrew Cody was one of Australia's leading opal authorities and made numerous contributions to the industry. Photo by Tao Hsu.

For more than 50 years, Cody worked tirelessly to promote Australian opal across the global gem industry, leaving an enduring legacy. We extend our condolences to his family and friends.